SPATIOTEMPORAL MONITORING OF THERMAL ENVIRONMENT IN ISFAHAN METROPOLITAN AREA

M. Bozorgi [1]*, F. Nejadkoorki [2]

[1] Dept. of Environmental Science, Yazd University, Yazd, Iran, mahsabozorgi@stu.yazd.ac.ir
[2] Dept. of Environmental Science, Yazd University, Yazd, Iran, f.nejadkoorki@yazd.ac.ir

Commission VI, WG VI/4

KEY WORDS: Land surface temperature, Urban heat island, Thermal environment, Land cover change, Landsat, Iran

ABSTRACT:

Urban Heat Island (UHI) phenomenon is regarded as one of the most critical issues in cities caused by unsustainable urban development. UHI has significant effects on air quality and energy consumption of urban buildings and it directly affects life quality the citizens. The current study aims to analyze and evaluate the spatiotemporal changes of thermal environment in Isfahan Metropolitan Area (IMA), Iran, during 1998-2014 time profile. A mono-window algorithm was applied to extract Land Surface Temperature (LST) values from Landsat thermal bands (TM and OLI sensors). Temporal and spatial changes in IMA's thermal environment were then analyzed using statistical methods, Mann-Kendall analysis and Urban-Heat-Island Ration Index (URI). Results indicated LST in IMA is of an increasing trend and the intensity of this trend is mainly concentrated in northwest and northeast of the city and around Zayandeh-Rood River in the south. This arrangement of UHI distribution is primarily due to compact and high-density patterns of city development in its boundaries, destruction of Zayandeh-Rood riverine ecosystem and its drying up during the last decade as well as excessive consumption of green covers by urban structures. Finally, it was concluded that the URI has witnessed an increasing trend from 0.25 in 1998 to 0.312 in 2014, which is in line with the spatiotemporal dynamics of thermal environment in the study location. The results of this study provide practical planning implications for identifying UHI hotspots in growing cities and optimization of green cover plantations to alleviate UHI effects in urban environments.

1. INTRODUCTION

1.1 Problem definition

Urbanization process is one of the most drastic forms of land-use transformation through which natural and semi-natural structures are converted into impervious surfaces. Such mechanism is associated with many feedbacks and feedback loops with surrounding ecosystems, which subsequently alter and modify the functioning of the cities and ecosystems (Gobakis et al., 2011; Wu 2014). Urbanization in this regard is a mechanism that occurs in urban boundaries and urban structures and transportation network occupy natural lands and green covers (Jing and Guangjin, 2011). This process is associated with many negative environmental consequences such as soil compaction, sealing, organic matter decline, biodiversity loss, air pollution, water contamination and the well-known Urban Heat Island (UHI) phenomenon (Oke, 1987; Rosenfeld et al., 1998; Voogt and Oke 2003). In urban environments, built-up structures are of higher thermal capacity (Taha 1997) and such locations can absorb higher temperature during daytime and release more heat fluxes during nighttime. Based on Oke (1995), UHI is referred to as the difference between urban and non-urban surrounding environment, which is a direct result of land-use conversion and human energy use. These differences are mainly due to land-use change caused by urbanization process that largely replaces soil and vegetative covers with impervious surfaces. These surface alternations consequently affect albedo, thermal capacity and heat conductivity over cities, which then modify thermal environment and micro-climate of the cities (Zhou et al. 2011). Higher temperatures resulted from UHI phenomenon can in turn lead to increased water consumption, elevated energy use and formation of secondary air pollutants such as ground level ozone, which causes respiratory problems to urban dwellers (Akbari et al. 2001). Therefore, improved understanding of UHI variability over temporal and spatial scales can assist urban planners to detect high-risk zones in cities and take appropriate preventive and restorative measures. In addition, monitoring spatiotemporal variability of UHI phenomenon can provide valuable planning implications for planting green covers and landscape design (Asgarian et al. 2015). Part of information for such purpose can be obtained from thermal remote sensing technology and this topic has also been an active research agenda in the literature, which attracted considerable attention from scholars in different parts of the world.

1.2 Literature review

Previous UHI studies have mainly concentrated on the effects of land-use composition and configuration on land surface temperature (LST) and remotely sensed data has been largely employed to evaluate LST patterns and UHI spatial distributions. Amiri et al. (2009) conducted a temporal study to analyze the relationships between different land-use categories and LST patterns. In this regard, the temperature vegetation index (TVX) space was calculated to investigate the temporal variability of thermal data and vegetation cover. According to their results, temporal profile of cells in the TVX space indicated major proportion of changes due to urbanization were

* Corresponding author

detectable as pixels transformed from the low temperature-dense vegetation to high temperature-sparse vegetation condition in TVX space. In their review paper, Mirzaei and Haghighat (2010) reported that the UHI phenomenon is associated with considerable impacts on the buildings energy and outdoor air quality. In addition, a series of important topics such as treatment of radiation, effect of trees and pond and boundary condition to simulate the behavior of UHI were also discussed. In a further attempt, Zhou et al. (2011) analyzed the relationship between LULC patterns and LST with an emphasis on configuration metrics using correlation analyses and multiple linear regressions. They highlighted that composition of LULC categories is of higher explanatory power for describing LST variations, however, a wise selection of composition and configuration landscape metrics can be effectively used for urban planning and mitigation of UHI effects. Chakraborty et al. (2013) studied the temporal profile of heat flux values related to the urban and industrial areas in Delhi, India. They concluded that there is an increasing trend for heat flux values, and therefore, LST increase related to the anthropogenic and impervious surfaces.

Chen et al. (2014) evaluated the seasonal effect of urban vegetation and water bodies on urban cool islands (UCIs) at patch level. The results illustrated that spatial arrangement (size, edge, shape and connectivity) of urban green clusters are of meaningful effects on their adjacent UCIs in four seasons. Asgarian et al. (2015) also conducted a patch level analysis of the relationships between urban areas and green covers with UHI. They implemented a step-wise generalized additive modeling method to develop a multiple linear regression model, which found to be potential to approximately explain half of the UHI variations. Afrakhteh et al. (2016) conducted a scenario-based temporal study to analyze the effect of different urban growth strategies on thermal landscape of Falavarjan Township, Iran. They highlighted that compared to historical trends; the integrated urban-rural planning perspective is associated with an urban landscape in which rural areas have higher opportunities to grow, while the UHI effect is alleviated across the landscape. Similarly, Chen et al. (2017) investigated diurnal LST variations in urban areas through MODIS Aqua satellite images. They reported that diurnal LST shows an increasing trend with increase of urbanization. In other words, they indicated increasing diurnal LST variation in response to urbanization implies that urbanization is potential to yield a higher increase in urban heat absorption than in thermal inertia.

Considering the above-mentioned researches, some general study patterns can be detected. Firstly, majority of studies in this field adopted a statistic approach such that the UHI spatial variations over a specific node year were analyzed and temporal variations were largely ignored, which can provide improved planning implications. Besides, similar to static analysis of UHI, temporal studies mainly evaluated the relationships between land-use categories and LST distribution patterns. In other words, the dynamics of such relationships is main focus of such studies, while the dynamics of the city thermal environment is disregarded. Therefore, analyzing spatiotemporal variability of a city's thermal environment can provide additional level of knowledge regarding locations that are experiencing an increasing trend of LST. Based on such analysis, a city planner can effectively decide on optimized location of green cover plantations and alleviate the impact of UHI phenomenon over city. Such measures can finally result in improved life quality of urban citizens and more efficient use of water and energy.

1.3 Research objectives

Based on above-referred criticism, this study attempts to analyze the spatiotemporal variability of thermal environment in Isfahan Metropolitan Area (IMA), Iran. Specifically, the main objectives of this research are as follows:

- Temporal LST mapping and integrating LST layers of different node years;
- Detection of potential UHI hotspots based on dynamics of thermal environment in IMA; and

Discussing the main planning implications derived from spatiotemporal analysis of IMA's thermal environment.

2. MATERIALS AND METHODS

2.1 Study area

Study area spans over IMA, central Iran. The area of research location is 115,567 ha bounded between 51˚ 26′ 27″ and 51˚ 49′ 58″ eastern longitude and 32˚ 40′ 49″ and 32˚ 32′ 38″ northern latitude (Figure 1). The IMA is of arid and semi-arid climatic conditions (Falahatkar et al., 2011) and average elevation is 1,575 m above the sea level. Annual mean, minimum and maximum air temperature of the study area are respectively 17.2, 24.18 and 10.18 ℃ (Isfahan Meteorological Organization, 2014). Zayandeh-Rood River crosses the middle of the city and Soffeh Mountain characterizes the main topography of the location in the south.

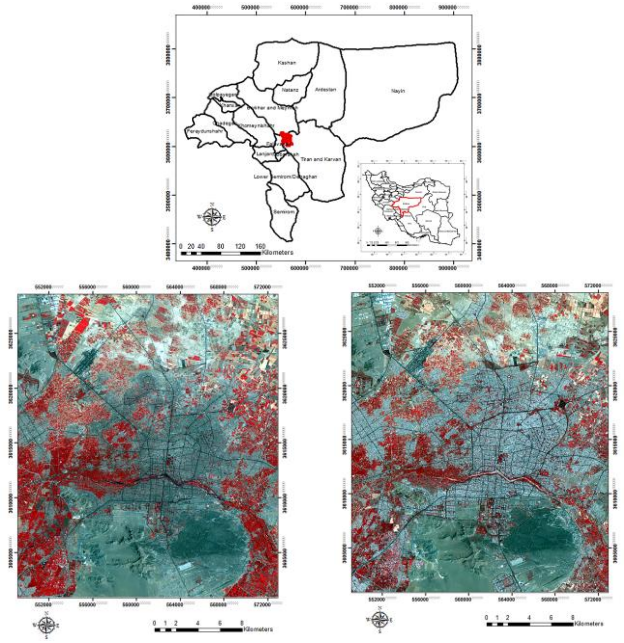

Figure 1. False color composite images demonstrating the location of study area across Isfahan Province and its spatial dynamics between (a) 1998 and (b) 2014

2.2 Data pre-processing

In this study, Landsat satellite images of the years 1998 (TM) and 2014 (OLI) were implemented for LST retrieval. Satellite data were firstly controlled in terms of radiometric, atmospheric and geometric corrections. In this regard, auxiliary data such as meteorological dataset obtained from the Isfahan Meteorological Organization (IMO), transportation network of the study area and field investigation data were used to ensure accuracy of the digital images.

2.3 Temporal LST retrieval

Bi-temporal (1998 and 2014) LST layers were generated applying the mono-window algorithm (Liu et al. 2011; Wang et al. 2015). On this basis, ground emissivity, atmospheric transmittance and effective mean atmospheric temperature are three essential parameters to retrieve LST (Qin et al., 2001). In order to calculate atmospheric transmittance and effective mean atmospheric temperature, two meteorological parameters including water vapor content and the near surface air temperature were carefully checked at the time of satellites overpass. Furthermore, emissivity was estimated using NDVI (Normalized Difference Vegetation Index) for different land surfaces. All other required data were obtained through the imagery metadata for both OLI and TM sensors. By the aim of brevity, the overall process of LST retrieval in this study is summarized in figure 2.

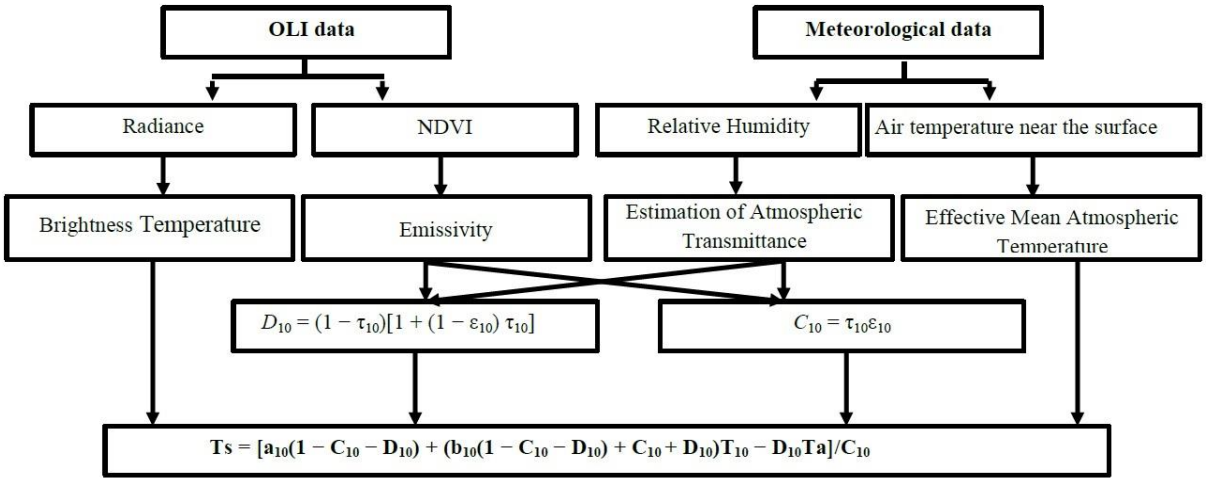

Figure 2. Mono-window algorithm flowchart for land surface temperature retrieval from Landsat satellite images

3. LST NORMALIZATION

In order to establish a basis for logical comparison of bi-temporal LST layers, the effects of time difference was removed applying the minimum and maximum temperature method (Xunqiang et al., 2011):

$$N_i = \frac{Ts_i - Ts_{min}}{Ts_{max} - Ts_{min}} \quad (1)$$

where Ni is the normalized LST image, Tsi indicates the LST value of a corresponding pixel, Tsmin and Tsmax are the minimum and the maximum LST values within raster space, respectively.

3.1 LST classification scheme

Bi-temporal normalized LST layers were classified using the mean-standard deviation method (Xu and Chen, 2004; Songlin and Tianxin, 2009). Accordingly, the LST layers were categorized into five classes of low temperature area, secondary low temperature area, medium temperature area, secondary high temperature area, and high temperature area. Numerical details regarding the classification scheme are provided in Table 1.

Table 1 LST classification scheme based on mean-standard deviation method (in this table Ts, μ and std respectively indicate normalized LST value, mean and standard deviation)

Temperature classification	Category interval
High temperature	$Ts > \mu + std$
Secondary high temperature	$\mu + 0.5std < Ts \leq \mu + std$
Medium temperature	$\mu - 0.5std \leq Ts \leq \mu + 0.5std$
Secondary low temperature	$\mu - std \leq Ts < \mu - 0.5std$
Low temperature	$Ts < \mu - std$

3.2 Mann-Kendall trend test

Mann-Kendall is a non-parametric test, which is employed to determine the presence and significance of a trend in the thermal environment of IMA. This method also estimates the starting point of a trend and sharp transitions in the thermal environment (Tayanç et al. 1997). Based on Mann-Kendall method, bi-temporal LST data are enumerated. For each element yi, the number of ni of elements yj preceding it (i > j) is calculated such that yi > yj. The t test is then calculated through the following formula:

$$t = \sum_i n_i \quad (2)$$

and referring to null hypothesis, t is distributed approximately normal with an expected value and variance (for more explanations in this regard readers are referred to Tayanç et al. 1997).

If a trend is present, the null hypothesis is rejected based on high values of |u (t)| according to the following equation:

$$u(t) = \frac{|t - E(t)|}{\sqrt{var(t)}} \quad (3)$$

if ut > 0, it indicates there is a positive trend and if ut < 0, it means there is a negative trend in LST values. The significance level is based on 95% (±1.96).

3.3 Urban-Heat-Island Ration Index (URI) calculation

URI (Xu and Chen, 2004) was considered as a measure to analyze temporal dynamics of the thermal environment in IMA during 1998-2014 time profile. The URI is calculated according to the following equation:

$$URI = \frac{1}{100m}\sum_{i=1}^{n} w_i p_i \quad (4)$$

where m is the number of normal LST categories (here is five), n refers to the number of LST categories that are of values higher than normal LST category (here the fourth and fifth categories have a higher temperature compared to third category which is of a normal temperature), w_i is the weighted value of LST categories that are higher than normal LST and p_i is the area percentage of categories that are of higher values than normal LST to the study area.

4. RESULTS AND DISCUSSION

Bi-temporal LST mapping (Figure 3) indicated the lowest and the highest LST for 1998 were 19 °C and 50 °C, respectively, while these values were correspondingly 28 °C and 57 °C in 2014. Such pattern of LST change demonstrates 9 °C increase for the minimum and 7 °C increase for the maximum temperature, which can be considered as a major concern in the region. Statistical parameters derived from LST layers are given in Table 2.

Table 2. Descriptive statistical parameters derived from resultant land surface temperature layers

Year	Minimum	Maximum	Mean	Std
1998	19.13	49.96	36.08	4.52
2014	27.68	57.41	43.86	4.78

The LST mean in the studied course of time has risen dramatically, from 36.08 °C in the beginning to 43.68 °C in 2014, (Table 2).

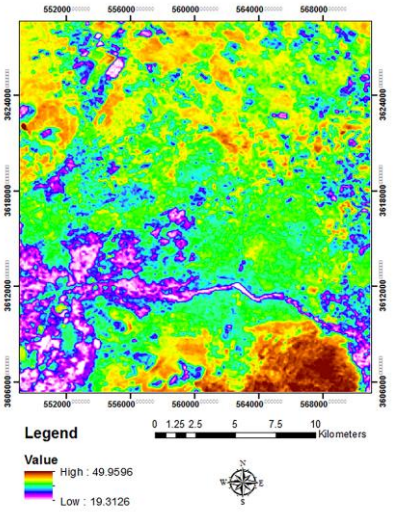

(a)

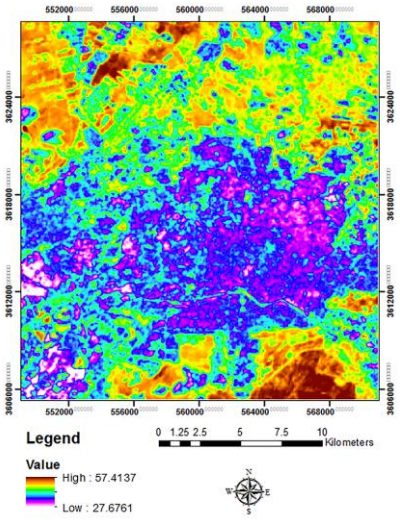

(b)

Figure 3. Land surface temperature layers for (a) 1998 and (b) 2014 node years

As it is illustrated in figure 3, the river bank LST has changed significantly during the course. In the image related to 1998, LST difference among urban versus the river and its green bank area is high. Whereas, in 2014, the river bank LST is the same as urban area. Moreover, some spots with high LST have been emerged in the dried river bed. Also, some spots with high LST have appeared in the north of the studied area, in 2014.

4.1 LST classification

For analyzing LST dynamics from 1998 to 2014, normalized LST maps were classified based on mean-standard deviation method. Low temperature class was considered as very cool locations and the high temperature class was regarded as the city's hotspot. Consequently, UHI hotspots were detected across the IMA (Figure 4). In addition, Table 3 shows the areal change of each LST class in the study area during 1998-2014 timespan. Areas of category five LST are considered as UHI due to their high temperature.

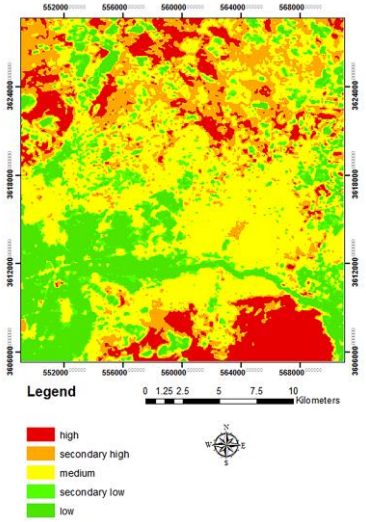

(a)

Table 3 Area of each land surface temperature category in 1998 and 2014 node years

LST classification	1998		2014	
	area (m^2)	Proportion (%)	area (m^2)	Proportion (%)
Low temperature area	78981718.69	15.49	87765677.35	17.21
Secondary low temperature area	48910639.2	9.59	105601840.6	20.71
Medium temperature area	226054570.2	44.33	145314242.4	28.50
Secondary high temperature area	88615492.77	17.38	69827970.25	13.69
High temperature area	67310079.14	13.20	101362769.4	19.9
Total	509872500	100	509872500	100

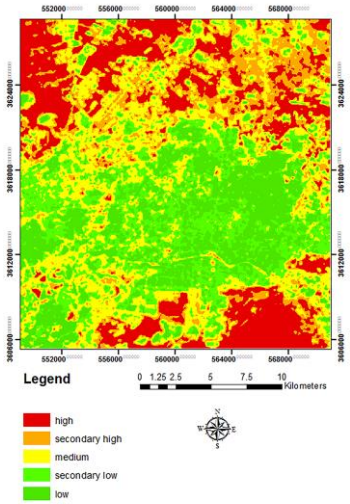

(b)

Figure 4. Classified land surface temperature layers for (a) 1998 and (b) 2014 node years

As it is illustrated in the figure 4, the temperature pattern in both images are different. The first category (low) shows the coolest areas. In the image related to 1998, Zayandeh-Rood River and its banks are classified in this category, despite the fact that in the image related to 2014, urban areas are classified in this category. In hot and arid regions, like the studied area, the suburb is covered with barren lands, and for the same reason, the suburbs has higher LST in regard with the urban areas.

The fifth category (high) shows UHI, and in both images UHI has expanded in barren lands and salty areas in suburban part. The results of Table 3 demonstrate that the area of high temperature class increased approximately 7% and the area of the medium temperature class decreased by 16%. Furthermore, areas of low temperature and secondary low temperature classes have been unexpectedly increased**.**

4.2 Analyzing the dynamics of thermal environment in IMA

In order to evaluate changes in UHI from 1998 to 2014, a post-classification method was applied. The results of such evaluation of changes in LST are shown in figure 5 and Table 4.

Fig. 5 Cross-tabulated land surface temperature layers (1998-2014) and mutual exchanges between different temperature categories in Isfahan Metropolitan Area

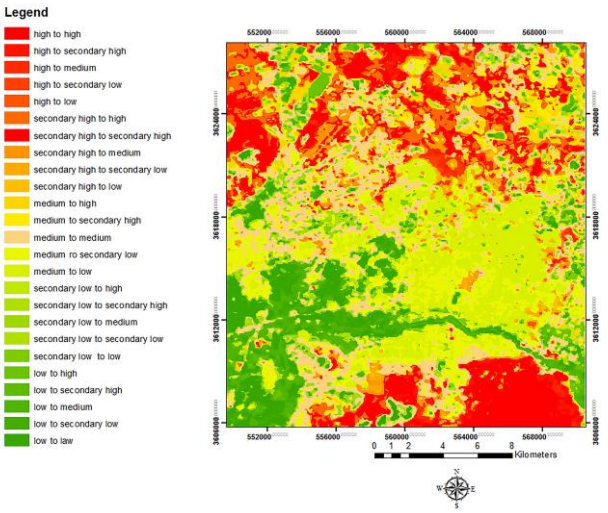

As it can be seen in Table 4, approximately 65% of the classified pixels in the Low category has moved to higher temperature categories from 1998 up to 2014. And, approximately 50% of the classified pixels in the Secondary low category has moved to higher temperature categories from 1998 up to 2014.

According to Table 2, minimum LST value has increased from 19.3 °C in 1998 to 27.8 °C in 2014. Based on 1998 LST layer, cooler areas in IMA are largely correlated with the location of Zayandeh-Rood River. In addition, green covers also demonstrate higher spatial extent and densities in the vicinity of Zayandeh-Rood River, which had a significant contribution in alleviating UHI effects over the IMA. Similarly, maximum LST value has increased from 50 °C in 1998 up to 57.4 °C in 2014 (Table 2). In both years, the maximum LST values are recorded within rock formations in southern part of the study area.

UHI effects are tractable in northern IMA in 2014, which is mainly the result of industrialization and conversion of agricultural fields to salty lands in this part of study area.

4 Mutual exchanges (%) between different land surface temperature categories during 1998-2014 time profile

1998 / 2014	High	Secondary high	Medium	Secondary low	Low
High	72.189	32.517	6.834	8.021	5.765
Secondary high	14.242	28.289	11.646	9.318	5.494
Medium	9.763	25.888	31.707	42.063	29.498
Secondary low	3.101	10.265	27.324	26.864	24.623
Low	0.705	3.042	22.489	13.734	34.619

Besides, UHI effects can also be observed in eastern IMA, which is mainly due to removal of green convers (Figure 3).
Based on figure 5, considerable changes of UHI phenomenon appeared to be around the city center. In this regard, according to Table 4, LST values were decreased in 171.81 km2 (36.53%) of the study area, while LST values increased over 150.20 km2 (32%) of the study area. LST values did not change for an area of 148.31 km2, which equals 31.53% of the total study area.

4.3 LST trend analysis

In this study, the Mann-Kendall methodology was used to analyze the LST trend in IMA. Figure 6 provides an illustration of thermal environment dynamics in the study area.

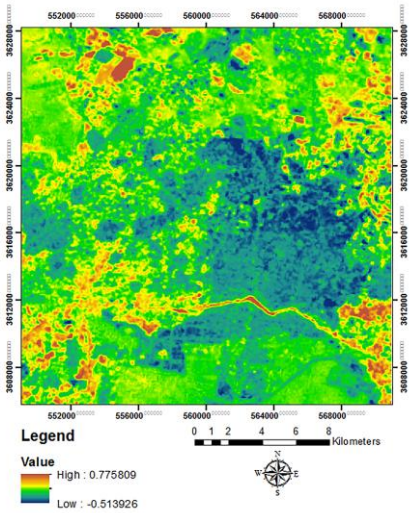

Figure 6. Pixel-based spatiotemporal dynamics of land surface temperature in Isfahan Metropolitan Area during 1998-2014 time profile

Based on figure 6, areas with biggest change in LST values are of scores closer to 1 and areas with minimum change in LST values are of scores closer to -1. Figure 5 demonstrates that surrounding areas compared to central locations have experienced an increasing LST trend and the intensity of this trend is higher in northwest and northeast of the research location. Furthermore, the margins of the Zayandeh-Rood seasonal river also observed drastic changes in LST. It represents the impact of the urban development and land-use changes on the spatial changes of UHI in IMA from 1998 to 2014.
In addition Zayandeh-Rood seasonal river bed shows a drastic LST trend. The river in 2014 was dried up and this matter indicates that the river has a significant impact on the thermal environment of IMA. In this study in addition to analysis and evaluation of UHI spatiotemporal dynamics, evaluation of UHI temporal change shows the URI index has increased from 0.25 in 1998 to 0.312 in 2014.

4.4 3.4 Planning implications

Analyzing spatiotemporal dynamics of thermal environment in IMA provides valuable planning implications for informed decision making and effective management in this region. Based on URI values distribution (Figure 6), river bank of Zayandeh-Rood and northwest and northeast of the study area have experienced more drastic process of LST intensification, which can potentially lead to formation of new UHI centers. In this regard, it is should be mentioned that Zayandeh-Rood riverine ecosystem has largely been destructed during the land decade such that this process has resulted in total drying of this river and water flow is only available through a very limited period during the year and . Therefore, conservation of water bodies within interior urban environments and rehabilitation of Zayandeh-Rood River ecosystem can largely alleviate thermal environment of the city and modifies micro-climate in IMA. In this case, construction of artificial water bodies near to detected UHI hotspots can largely reduce the intensity of such phenomenon over the entire of the city.
Referring to figures. 5 and 6, newly constructed urban structures within urban boundaries have witnessed higher rates of LST increase. Simply put, urban boundaries are the locations that experienced higher level of dynamics from low temperature LST categories to high temperature categories. This matter reflects the local characteristics of the study area. Specifically, due to factors such as available vacant lands and lack of effective regional regulations (Afrakhteh et al. 2016), cities in central Iran tend to expand their boundaries towards immediate vacant lands and agricultural fields, and therefore, cities experience a more compacted and connected pattern of urban growth in this region. Such pattern of urban development leads to construction of buildings in higher densities, and thus, these locations are potential to form future UHI centers. In addition, urban growth is mainly associated with consumption of green covers in central Iran (Asgarian et al. 2015), which can further exacerbates UHI formation conditions. Therefore, decentralized urban planning (Sakieh et al. 2015) could be considered as an available option for conservation of green covers and reduction of UHI effects. On the basis of decentralized urban planning, construction of urban structures is occurred in more dispersed patterns; however, spatial configuration of urban patches is regulated in terms of land suitability parameters for urban construction activities. In other words, a polycentric pattern of growth instead of high-density urban development is emphasized and urban vegetation covers under such pattern have a better chance to survive for encroachment of built-structures. As indicated in previous studies (Sakieh et al. 2015; Afrakhteh et al. 2016; Sakieh et al. 2017), such pattern of urban growth allocation is associated with many ecological benefits such as lower LST values, calmer landscapes and higher land

potential for urban construction activities and biodiversity conservation (Goodarzi et al. 2017). In addition, Afrakhteh et al. (2016) highlights this strategy under the concept of smart rural development in central Iran. They argue that activation of rural growth cycles and minimization of growth rates in major urban centers can lead to construction of a cooler landscape, in which both urban and rural environments are allowed to continue their growth profile under a controlled and planned situation. In addition, Afrakhteh et al. (2016) report that physical size of the rural and small urban cores is the most powerful variable in describing thermal environment in a city in central Iran. Therefore, area monitoring of newly constructed urban centers under the polycentric (or decentralized) planning strategy is recommended to prevent formation and undesirable effects of UHI phenomenon in central Iran.

5. CONCLUSIONS

This paper explained application of Landsat imagery to monitor thermal environment dynamics in a metropolitan area. Analysis and evaluation of UHI spatiotemporal changes in IMA revealed that the pattern of LST has been changed during the last two decades. Results indicated LST in IMA is of an increasing trend. It had 9 °C increase for the minimum and 7 °C increase for the maximum temperature and the intensity of this trend is mainly concentrated in northwest and northeast of the city and around Zayandeh-Rood River in the south. This difference is mainly correlated with increasing area of high temperature LST category. Temporal evaluation of UHI change indicates that the URI index has increased from 0.25 in 1998 to 0.312 in 2014. Results also demonstrated that the IMA not only witnessed an increase in the area of UHI but also the intensity of UHI has been surged substantially between 1998 and 2014. Finally, using developed methods for LST retrieval (Jahani, Mohammadi, 2014) is suggested, and also it is recommended that future research efforts study the causes of UHI dynamics especially in locations where there is higher densities of urban structures and higher intensities of anthropogenic activities.

6. REFERENCES

Afrakhteh, R., Asgarian, A., Sakieh, Y., Soffianian, A., 2016. Evaluating the strategy of integrated urban-rural planning system and analyzing its effects on land surface temperature in a rapidly developing region. *Habitat International*, *56*, 147–156.

Akbari, H., Pomerantz, M., Taha, H., 2001. Cool surfaces and shade trees to reduce energy use and improve air quality in urban areas. *Solar Energy*, 70, 295–310.

Amiri, R., Weng, Q., Alimohammadi, A., Alavipanah, S., 2009. Spatial-temporal dynamics of land surface temperature in relation to fractional vegetation cover and land use/cover in the Tabriz urban area, Iran. *Remote Sensing of Environment*, 113, 2606–2617.

Asgarian, A., Amiri, B. J., Sakieh, Y., 2015. Assessing the effect of green cover spatial patterns on urban land surface temperature using landscape metrics approach. *Urban Ecosystems*, 18(1), 209–222.

Chakraborty, S. D., Kant, Y., Mitra, D., 2013. Assessment of land surface temperature and heat fluxes over Delhi using remote sensing data. *Journal of Environmental Management*, 148, 143–152.

Chen, A., Yao, X. A., Sun, R., Chen, L., 2014. Effect of urban green patterns on surface urban cool islands and its seasonal variations. *Urban Forestry and Urban Greening*, 13(4), 646–654.

Chen, Y., Chiu, H., Su, Y., Wu, Y., Cheng, K., 2017. Does urbanization increase diurnal land surface temperature variation? Evidence and implications. *Landscape and Urban Planning*, 157, 247–258.

Falahatkar, S., Soffianian, A. R., Khajeddin, S. J., Ziaee, H. R., Ahmadi Nadoushan, M., 2011. Integration of Remote Sensing data and GIS for prediction of land cover map. *International Journal of Geomatics and Geosciences*, 1, 847–864.

Gobakis, K., Kolokotsa, D., Synnefa, A., Saliari, M., Giannopoulou, K., Santamouris, M., 2011. Development of a model for urban heat island prediction using neural network techniques. *Sustainable Cities and Society*, 1, 104–115.

Goodarzi, M. S., Sakieh, Y., Navardi, S., 2017. Measuring the effect of an ongoing urbanization process on conservation suitability index: integrating scenario-based urban growth modeling with conservation assessment and prioritization system (CAPS). *Geocarto International*, doi: 10.1080/10106049.2017.1299799.

Isfahan Meteorological Organization., 2014. Annual report of Isfahan Meteorology, Isfahan Meteorological Organization, Iran, http://www.esfahanmet.ir/.

Jahani, B., Mohammadi, B., 2018. A comparison between the application of empirical and ANN methods for estimation of daily global solar radiation in Iran. Theoretical and Applied Climatology, https://doi.org/10.1007/s00704-018-2666-3.

Jing, J., Guangjin, T., 2011. Analysis of the impact of Land use/Land cover change on Land Surface Temperature with Remote Sensing. Paper presented at the International Society for Environmental Information Sciences 4101 Annual Conference (ISEIS).

Liu, L., Zhang, Y., 2011. Urban Heat Island Analysis Using the Landsat TM Data and ASTER Data: A Case Study in Hong Kong. *Remote Sensing*, 3, 1535–1552.

Mirzaei, P. A., Haghighat, F., 2010. Approaches to study urban heat island—abilities and limitations. *Building and Environment*, 45(10), 2192–2201.

Oke, T. R., 1987. Boundary layer climates. (London and New York: Methuen & Co)

Oke, T. R., 1995. The heat island of the urban boundary layer: Characteristics, causes and effects. In J. E. Cermak (Ed.), Wind climate in cities (pp. 81–107). Netherlands: Kluwer Academic Publishers.

Qin, Z., Karnieli, A., Berliner, P., 2001. A mono-window algorithm for retrieving land surface temperature from Landsat TM data and its application to the Israel-Egypt border region. *International Journal Remote Sensing*, 22, 3719–3746.

Rosenfeld, A. H., Akbari, H., Romn, J. J., Pomerantz, M., 1998. Cool communities: strategies for heat island mitigation and smog reduction. *Energy and Buildings*, 28, 51–62.

Sakieh, Y., Jaafari, S., Ahmadi, M., Danekar, A., 2017. Green and calm: Modeling the relationships between noise pollution propagation and spatial patterns of urban structures and green covers. *Urban Forestry & Urban Greening*, doi: 10.1016/j.ufug.2017.04.008

Sakieh, Y., Salmanmahiny, A., Jafarnezhad, J., Mehri, A., Kamyab, H., Galdavi, S., 2015. Evaluating the strategy of decentralized urban land-use planning in a developing region. *Land Use Policy*, 48, 534–551.

Songlin, C., Tianxin, W., 2009. Comparison Analyses of Equal Interval Method and Mean-standard Deviation Method Used to Delimitate Urban Heat Island. *Journal of Geoinformation Science*, 11, 146–150.

Taha, H., 1997. Modeling the impacts of large-scale albedo changes on ozone air quality in the South Coast air basin. *Atmosphere Environment*, 31, 1667–1676.

Tayanç, M., Karaca, M., Yenigün, O., 1997. Annual and seasonal air temperature trends patterns of climate change and urbanization effects in relation with air pollutants in Turkey. *Journal of Geographical Research*, 102(D2), 1909–1919.

Voogt, J. A., Oke, T. R., 2003. Thermal remote sensing of urban climates. *Remote Sensing of Environment*, 86, 370–384.
Wang, F., Qin, Z., Song , C., Tu, L., Karnieli, A., & Zhao, S. (2015). An improved mono-window algorithm for land surface temperature retrieval from Landsat 8 thermal infrared sensor data. *Remote Sensing*, 1, 4268–4289.

Wu, J. G., 2014. Urban ecology and sustainability: The state-of-the-science and future directions. *Landscape and Urban Planning*, 125, 209–221.

Xu, H., Chen, B., 2004. Remote sensing of the urban heat island and its changes in Xiamen City of SE China. *Journal of Environmental Sciences*, 16, 411–418.

Xunqiang, M., Cheng, C., Zhai, F., Li, H., 2011. Study on temporal and spatial variation of the urban heat island based on Landsat TM/ETM+ in central city and Binhai New Area of Tianjin. Paper presented at the Multimedia Technology (ICMT), 2011 International Conference on. 26–28 July 2011.

Zhou, W., Huang, G., Cadenasso, M. L., 2011. Does spatial configuration matter? Understanding the effects of land cover pattern on land surface temperature in urban landscapes. *Landscape and Urban Planning*, 102(1), 54–63